Published in: Materials Science and Engineering A 386(2004) 156-163

The assessment of GPB2/S" structures in Al-Cu-Mg alloys

S.C. Wang†*, M.J. Starink
Materials Research Group, School of Engineering Sciences,
The University of Southampton, SO17 1BJ
†Also at: Electron Microscopy Centre, Faculty of Engineering and Science,
The University of Southampton, SO17 1BJ

Abstract

Based on experimental data presented in the literature, we propose a new structure for GPB2/S" with the composition of $Al_{10}Cu_3Mg_3$, which is aluminium-rich compared to S phase (Al_2CuMg). The proposed structure is coherent with the f.c.c. Al matrix, is formed by the replacement of some Al atoms with Cu/Mg, and has orthorhombic structure (space group Imm2) with lattice parameters a = 0.405 nm, b = 1.62 nm and c = 0.405 nm. Simulated high resolution electron microscopy images and simulated diffraction patterns are compared with experimental data on a range of Al-Cu-Mg alloys. A good correspondence is found.

Key words: GPB; S"; HREM; Diffraction; Al-Cu-Mg alloy

*Corresponding author, Tel: 0044 23 8059 5101; fax: 0044 23 8059 2236
E-mail address: Hwangs@soton.ac.uk (Shuncai Wang)

Published in: Materials Science and Engineering A 386(2004) 156-163

1. Introduction

In the early 50s, Bagaryatsky [T1] first proposed a 4-stage precipitation sequence for the ageing of Al-Cu-Mg alloys:

$$\text{SSS} \rightarrow \text{GPB zone} \rightarrow \text{S''(GPB2)} \rightarrow \text{S'} \rightarrow \text{S} (CuMgAl_2).$$

where SSS stands for supersaturated solid solution and GPB stands for Guinier-Preston-Bagaryatsky [2]. In fifty years of research on these phases substantial information on their structures has been obtained. Recent studies [e.g. 3] ruled out the existence of an independent S' which is now regarded as continuous rather than distinct to S phase. A few structures of S phase were reported [4-7], but the most accepted structure for S phase appears to be the one proposed by Perlitz and Westgren [4] that has a Cmcm structure with lattice parameters a = 0.400 nm, b = 0.923 nm, c = 0.714 nm and forms as laths on {210}Al habit planes and elongates along <100>Al. The orientation relationship between S and aluminium matrix is [1]:

$$[100]_{Al} // [100]_S, \ [02\bar{1}]_{Al} // [010]_S, [012]_{Al} // [001]_S \qquad (1)$$

Unlike GP (Guinier-Preston) zones in Al-Cu based alloys, GPB zones have not been unambiguously evidenced by selected area electron diffraction (SAD) in transmission electron microscopy (TEM) or by phase contrast in high resolution electron microscopy (HREM). This might be related to limited contrast of GPB zones, which could be due to the size effects of Cu (radius=0.128 nm) and Mg atoms (radius=0.160 nm) counteracting each other, however the most likely explanation for the absence of characteristic streaking in SAD is that Cu and Mg solute atoms cluster in a random manner rather than in certain specific planes. Recent work [8,9] using three-dimensional atom-probe (3DAP) shows that Cu-Mg clusters appear during initial ageing. Formation of Cu-Mg clusters is responsible for the rapid hardening after quenching, and this stage accounts for approximately 60% of the total hardness increase during ageing [8,10].

A range of structures have been proposed for GPB, GPB2 and S'', as shown in Table 1. The S'' structure proposed by Cuisiat et al. [11] and the GPB structure proposed by Wolverton [12] are illustrated in Fig. 1. These structures were suggested by the respective researchers to explain HREM, TEM, SAD or X–ray diffraction (XRD) observations, but none has been tested through comparison with data from several techniques or diffraction data from several orientations. None of the structures

in Table 1 are considered to be unambiguously proven, and some researchers [9,13,14] have pointed out the weakness of some of the data used to support a distinct S"/GPB2 phase. The present authors [15] have recently proposed a new structure for S"/GPB2. The purpose of this paper is to fully examine relevant published HREM and SAD data, and consider how it can be explained by the recently proposed structure [15].

Table 1 Previous reported and proposed structures for GPB and S"

Crystallographic Structure	Composition	Experimental data supporting model	Structure name	References
Short range ordering of one Cu+Mg layer and several Al layers along the $\{100\}_{Al}$ planes	Al_xCuMg	XRD	GPB	[1]
Monoclinic, a = 0.400 nm, b = 0.925 nm, c = 0.718 nm, α=88.6º	Al_2CuMg	XRD	S"	[16]
Monoclinic, a = 0.32 nm, b = 0.405 nm, c = 0.254 nm, β = 91.7º.	unknown	HREM	S"	[17]
Orthorhombic, a = 0.405 nm, b = 0.906 nm and c = 0.725 nm	Al_2CuMg	proposed	GPB	[5]
Orthorhombic, a = 0.405 nm, b = 0.405 nm and c = 0.81 nm, Imm2	Al_2CuMg	TEM	S"	[11]
Orthorhombic, a = 0.405 nm, b = 0.405 nm and c = 0.81 nm, Cmmm	Al_2CuMg	FPTEC	GPB	[12]
Tetragonal, CuAuI type, a=0.47 nm, c= 0.4 nm	Al_2CuMg	XRD	GPB	[18]
Tetragonal a = 0.55 nm, c = 0.404 nm	Al_2CuMg	XRD	GPB	[2]
Tetragonal, a = 0.58 nm, c = 0.808 nm	Al_xCuMg	TEM	S"	[19]
Cubic, a = 0.827 nm	$Al_5Cu_5Mg_2$	XRD	S"	[2]

XRD – X-ray diffraction
FPTEC - First-principles total energy calculations

2. Experimentally observed structures and diffraction patterns

In HREM work on an Al-2.03 wt.% Cu-1.28 wt.% Mg alloy that was solution treated and aged at 200ºC for 4 h, Charai et al. [17] found the extra reflections A-D/A'-D' (Fig. 2b) by Fourier transformations (FT) from the rectangular region I indicated in Fig. 2(a), whereas these extra diffractions cannot be observed in Al matrix from the rectangular region II as shown in Fig. 2c. These authors measured the spacings of OA/OD (OA'/OD') and OB/OC (OB'/OC') (see Fig. 2) to be 0.25 and 0.32nm, which are close to the spacing of $\{112\}_S$ and $\{111\}_S$ respectively. As $\{111\}_S$ should be not observed in $[001]_{Al}$ according to the orientation relationship between S phase Al matrix (Orientation 1), and none of the structures reported prior to the work of Charai et al. [17] could explain these reflections, they attributed the FT to a new phase which would have a primitive monoclinic structure with a = 0.32 nm, b = 0.405 nm, c = 0.254 nm, β=91.7°. They termed it as S" phase. However, their suggested structure could not explain why one of these precipitates (region I of Fig. 2a) produced two sets of diffraction patterns in $[100]_{Al}$ (Fig. 2b), and no HREM simulation supporting such a structure was presented.

In analysing the available experimental diffraction and HREM data that could confirm the presence of a discrete second phase distinct from the S'/S phase, and akin to the S" phase identified in Ref [17], we found two studies. In recent HREM work on Al-0.4 wt.% Cu-3 wt.% Mg-0.12 wt.% Si (low Cu/Mg ratio) aged 8 h at 180ºC, Kovarik et al. [20] observed two types of precipitate variants. One gave the same FT as observed for a precipitate in the Al-2.03 wt.% Cu-1.28 wt.% Mg alloy studied by Charai et al. [17], the second variant had an FT consistent with a variant present in SAD patterns for an Al-0.6 wt.% Cu-4.2 wt.% Mg alloy aged at 180ºC for 34 h studied by Ratchev et al. [21]. These diffraction patterns are presented in Fig. 3: Fig. 3(a) presents the complex diffractions by FT from a large area which contains at least two S" variants in the Al-2.03 wt.% Cu-1.28 wt.% Mg aged at 200ºC for 4 h, and Fig. 3(c) shows the SAD pattern for the Al-0.6 wt.% Cu-4.2 wt.% Mg alloys (from [21]). (Note that in Ref. [8] the pattern was ascribed to an oxide layer with α– or γ-Al_2O_3 structure.). These observations suggest that the precipitates observed by the three groups of researchers [19-21] in Al-2.03 wt.% Cu-1.28 wt.% Mg aged at 200ºC for 4 h, Al-0.4 wt.% Cu-3 wt.% Mg-0.12 wt.% Si aged at 180ºC for 8 h and Al-0.6 wt.% Cu-4.2 wt.% Mg aged at 180ºC for 34 h are the same structure. Note

though that the three groups preferred differed names for the structure, naming them S" phase, GPB2 and 'disordered zones', respectively.

3. Interpretation of experimental data using reference structures

3.1. Attempt explanation based on the structure of S phase

As the diffraction patterns of Al-2.03 wt.% Cu-1.28 wt.% Mg aged at 200ºC for 4 h (Fig. 2b) are very similar to those of S phase, we need to consider the possibility that the reflections A-D/A'-D' are from a variant of S phase. There are 12 equivalent orientation relationships to orientation (1), and therefore 12 variants of S phase may precipitate from the Al matrix. Fig. 4 shows the calculated diffraction pattern from one of the S variants in $[001]_{Al}$ (indexed based on Gupta et al. [22]). Comparison between Figs. 2(b) and 4 shows that spots of A/A', D/D' in Fig. 2(b) are caused by $\{112\}_S$ reflections from one S variant, and the locations of B/B' and C/C' correspond to double diffractions [22]. However, Fig. 4 cannot explain the FT data of Charai et al. [17] because the B/B' and C/C' reflections in Fig. 2(b) cannot be caused by double diffractions in the FT on a 2-dimensional (2D) HREM image. Double diffractions can only arise from bulk samples in 3-dimension (3D). No match can be found between the experimental HREM images and images of S phase simulated using the EMS on-line software [23] (simulated images not presented). According to Shchegoleva and Buinov [], the S" phase is a slightly distorted S phase, and therefore their model cannot clarify the images and diffractions of Fig. 2 either.

3.2 Attempt explanation based on the structure of GPB2/S",GPB

To elucidate the HREM in Fig. 2(a), we performed simulations for the reported types of GPB2/S" [11,12] (the other reported GPB2/S" [2,19] structures could not be simulated as in those works atomic coordinates were not specified). However, none of the HREM simulation for the models [11,12] (using the EMS on line software [23] at 200 kV and Cs = 0.5 mm) was found to match Fig. 2(a). In attempting to explain the FT in Fig. 2(b), the structural factors for the above two structures were calculated based on the atomic coordinates and scattering amplitudes, and from that we could estimate the corresponding intensities of individual diffractions. Figs. 5(a) and 5(c) show the simulated diffraction patterns of one S" variant in a three-dimensional representation for the models of Cuisiat et al. [11] and Wolverton [12], respectively and Figs. 5(b) and 5(d) are the complex diffraction patterns combining all

the variants of GPB2/S" projected on $[001]_{Al}$ for the models of Cuisiat et al. [11] and Wolverton [12], respectively. None of these simulated patterns can explain the FT and SAD patterns as shown in Figs. 2 and 3.

4. Interpretation of experimental data using a new structure

Wolverton's [12] configuration for GPB zone (Fig. 1b) is a low energy configuration, and hence we have considered a new GPB2/S" structure constructed from elements of Fig. 1b. We constructed a new structure shown in Fig. 6(a) such that the pattern viewed along [001] resembles the patterns seen in the HREM image in Fig. 2a. Fig. 6(b) shows HREM simulated images along [001] in different thickness and defocuses, and it can be seen that for 2nm of thickness and defocus at 68 nm the simulated image matches well the experimental image in Fig. 2(a). The orientation relationship between GPB2/S" and Al matrix satisfies: $<100>_{GPB2/S"}$ // $<100>_{Al}$, $<010>_{GPB2/S"}$ // $<010>_{Al}$. On calculation of its structural factors, we can predict the diffraction patterns for all 6 independent variants of GPB2/S" precipitates in $[001]_{Al}$ as shown in Fig. 7. Combination of two variants (Figs. 7a, b) can explain the experimental data in Fig. 3(a), but no solution can be found to elucidate the pattern in Fig. 3(c). The structure also fails to produce a match with the FT one of the two variants of the precipitates observed by Kovarik et al. [20].

The structure of Fig. 6(a) has many Mg-Mg or Cu-Cu neighbours and thus large local lattice distortions may be introduced as a result of the different atomic sizes between Mg (0.320 nm), Cu (0.256 nm) and Al (0.286 nm). It is considered that such large distortions may not be accommodated unless very large strains are introduced. Thus a structure with fewer Mg-Mg and Cu-Cu nearest neighbours may be more stable, and we constructed an alternative model by interchanging Cu and Mg as shown in Fig. 8. This structure presents the same simulated HREM images along [001] as Fig. 6(b) and thus also fits the HREM image in Fig. 2(a). The corresponding diffraction patterns from six independent variants of GPB2/S" were predicted (figure not presented) but again no match was found to the pattern in Fig. 3(c) and also the FT of one of the two variants of the precipitates observed by Kovarik et al. [20], which is similar to Fig. 3(c), did not match.

To fit the diffraction pattern between the observation and simulation, we propose an alternative model in which the positions of Cu and Mg atoms are mixed 50%Cu/50%Mg as shown in Fig. 9(a). Its

composition $Al_{10}Cu_3Mg_3$ is between that of S phase (Al_2CuMg) and Cu-Mg clusters which have about 90% Al [24]. (Mixed occupancy also occurs in the GP2/θ" structure in Al-Cu alloys [25].) As shown in Fig. 9(a), this structure has no four-fold symmetry and the lattice parameters are a = 0.405 nm, b = 1.62 nm and c = 0.405 nm. The following reflection conditions should occur: {h00}: h=2n; {0k0}: k=2n; {00l}: l=2n; {hk0}: h+k=2n; {h0l}: h+l=2n; {0kl}: k+l=2n; {hkl}: h+k+l=2n. (n is integer). Thus the structure is orthorhombic with Imm2 space group [26].

Fig. 9(b) shows the corresponding HREM simulation images for a series of thickness and defocus combinations. We may see that simulated HREM in 4nm of thickness and defocus at 62 nm (Fig. 9b) fits the experimental image of Fig. 2(a) well. The calculated diffraction patterns for 6 independent GPB2/S" variants are shown in Fig. 10. Again, the combination of Figs. 10(a) and (b) fits well to the observed pattern (Fig. 3a). Furthermore, the combination of Figs. 10(c) and (d) fits well the SAD pattern in Fig. 3(c) and also fits the FT of both variants of the precipitates observed by Kovarik et al. [20]. Figs. 11(a-c) shows the complex reflections of all the variants of GPB2/S" projected on $[001]_{Al}$ based on the three structures shown in Figs. 6(a), 8 and 9(a).

In an additional analysis we carried out HREM and diffraction simulations for the structure in Fig. 9(a) with Cu:Mg ratios between 0:1 to 1:0. The results show small changes in HREM simulation with Cu:Mg ratio, and for all Cu:Mg ratios between 0.5:0.5 to 0.66:0.33, which corresponds to compositions $Al_{10}Cu_{3+x}Mg_{3-x}$ ($0 \le x \le 1$), a good fit with HREM and diffraction data was observed.

5. Discussion

Having obtained strong indications that a single GPB2/S" phase with structure in Fig. 9 is present in artificially aged Al-2.03 wt.% Cu-1.28 wt.% Mg, Al-0.4 wt.% Cu-3 wt.% Mg-0.12 wt.% Si and Al-0.6 wt.% Cu-4.2 wt.% Mg alloys, we analysed a range of published [24,27] and unpublished SAD data [28] of artificially aged Al-Cu-Mg alloys with significantly higher Cu contents. For a 2024 alloy (Al-4.2 wt.% Cu-1.5 wt.% Mg) aged at 150ºC for up to 2 days, patterns were observed that could not be fully explained by S phase. The $[001]_{Al}$ SAD pattern of a 2024 alloy aged at 150ºC for 12 h after solution treatment and 2% stretch is presented in Fig. 11(d). This stage of the ageing treatment corresponds to the final stages of the hardness plateau, before the increase in hardness leading up to the

peak hardness commences [24,27], and thus we would expect that very little S phase is present [27]. Even though the very fine precipitates cause the SAD pattern to be diffuse and no conclusive phase identification can be obtained from this data, it is clear that Fig. 11(c) fits well to Fig. 11(d). Therefore, this SAD data is also consistent with the structure of GPB2/S" in Fig. 9(a).

Finally, it needs to be pointed out that the present analysis of the available data leaves open the possibility that the proposed GPB2/S" phase may depend on alloy composition or that more than one structure could be responsible for the experimental data included in the present paper. Nevertheless, on the balance of evidence, it is probable that the data presented is related to the presence of one discrete phase with the structure presented in Fig. 9(a).

6. Conclusions

A new structure for GPB2/S" which is a discrete orthorhombic phase coherent with the matrix is proposed. Its composition $Al_{10}Cu_{3+x}Mg_{3-x}$ ($0 \leq x \leq 1$) is between that of S phase (Al_2CuMg) and Cu-Mg clusters which have about 90% Al. Observed HREM and SAD data for precipitates in Al-2.03 wt.% Cu-1.28 wt.% Mg aged at 200ºC for 4 h, Al-0.4 wt.% Cu-3 wt.% Mg-0.12 wt.% Si aged at 180ºC for 8 h and Al-0.6 wt.% Cu-4.2 wt.% Mg aged at 180ºC for 34 h matches HREM and SAD simulations for the proposed orthorhombic structure.

Acknowledgements

The authors are grateful to Prof. A. Charai and Dr P. Ratchev, who provided us Fig. 2, Fig. 3(a) and Fig. 3(c), respectively.

Published in: Materials Science and Engineering A 386(2004) 156-163

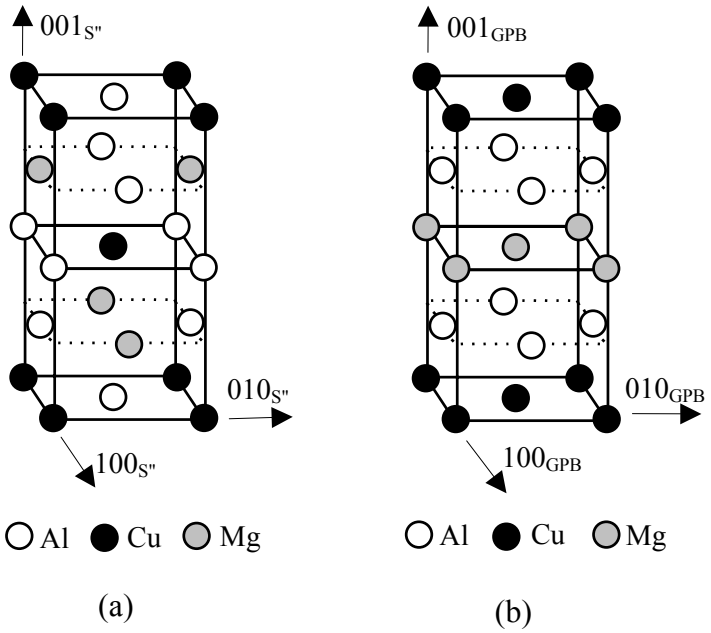

Fig. 1(a) The S" structure proposed by Cuisiat et al. [11]; (b) The GPB structure proposed by Wolverton [12].

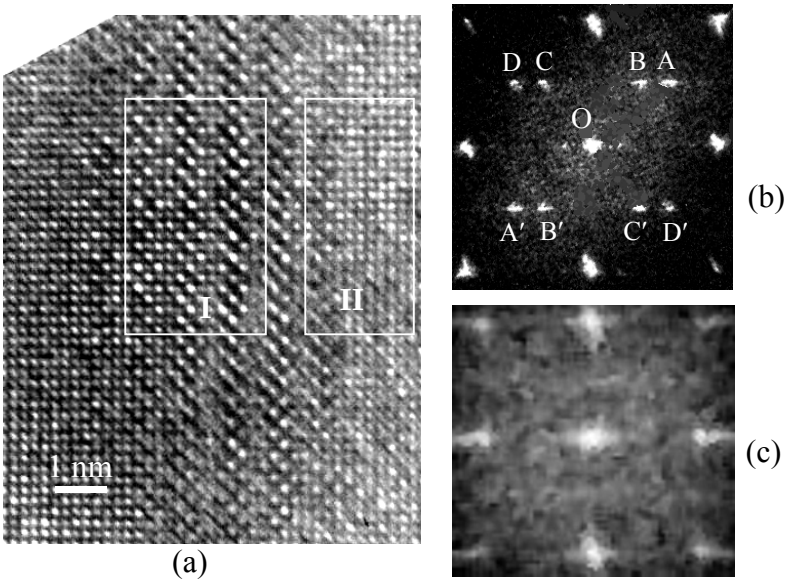

Fig. 2(a) HREM images in $[100]_{Al}$ of an Al-2.03wt%Cu-1.28wt%Mg alloy aged 200°C for 4h; (b) & (c) The Fourier transformed diffraction patterns corresponding to the rectangular regions I & II, respectively. (a and b from Ref. [17], by courtesy of Prof. A. Charai).

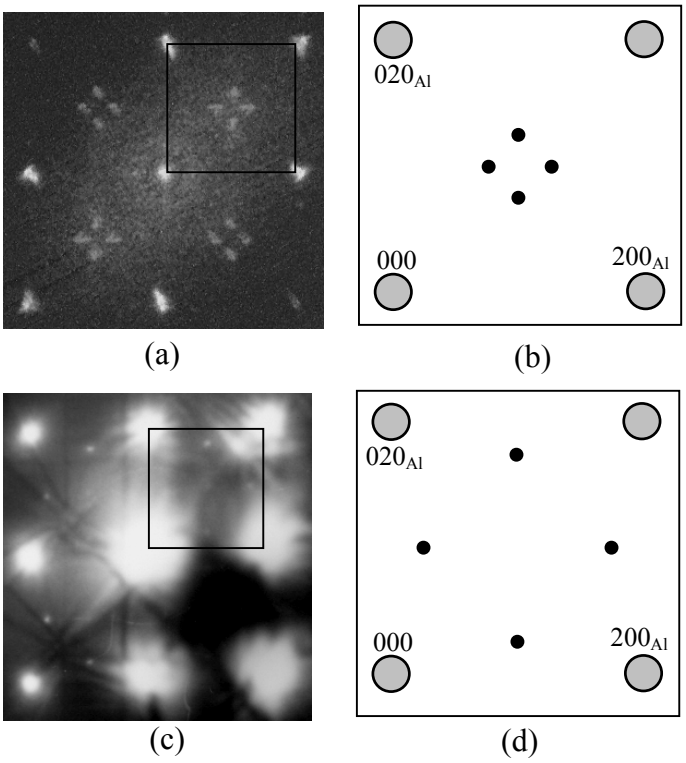

Fig. 3(a) The $[001]_{Al}$ diffraction pattern for S" from large area by Fourier transformation in an Al-2.03wt%Cu-1.28wt%Mg aged 200°C for 4h (from [17]); (b) The schematic diagram to Fig. 3(a); (c) The observed $[001]_{Al}$ diffraction pattern from the Al-0.6wt%Cu-4.2wt%Mg alloy aged at 180ºC for 34 h (from Ref. [21], by courtesy of Dr P. Ratchev); (d) The schematic diagram to Fig. 3(c).

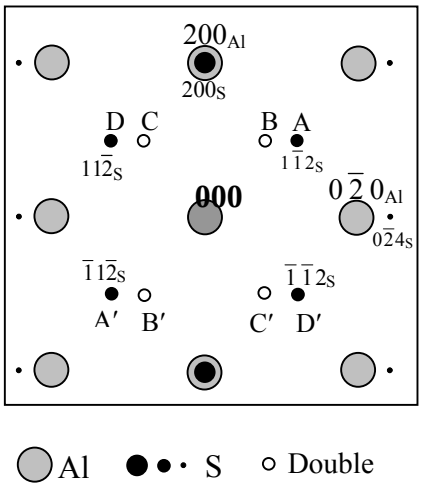

Fig. 4 The calculated diffraction pattern from one variant of S phase in $[001]_{Al}$ indexed according to work by Gupta et al. [22]. Sizes of the spots are proportional to the reflection intensities.

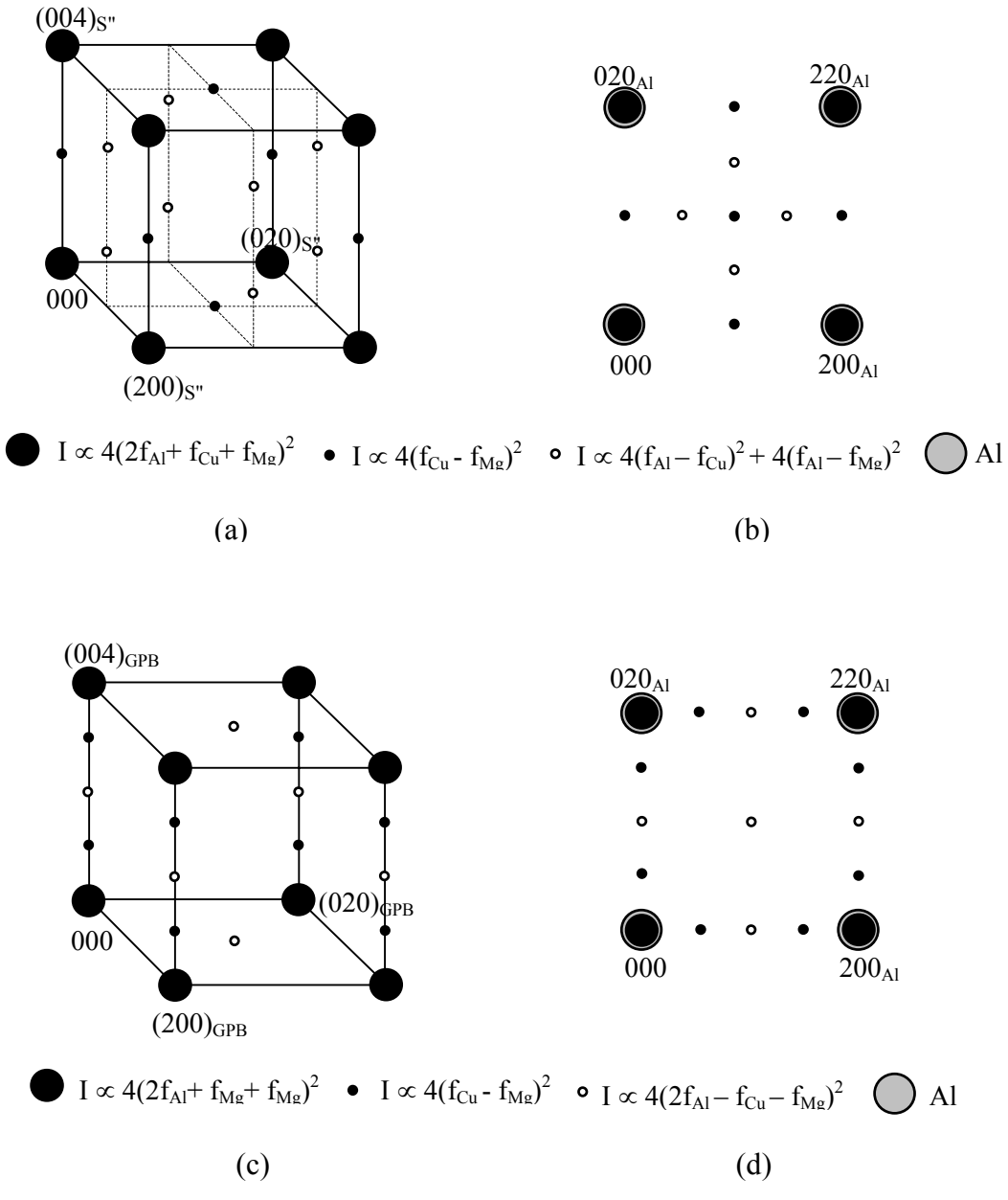

Fig. 5(a) Simulated diffraction patterns in three $<001>_{S"}$ zones based on the model of Cuisiat et al. [11] in Fig. 1(a); (b) Simulated diffraction patterns showing all 6 variants of the S" of Fig. 5(a) upon $[001]_{Al}$; (c) Simulated diffraction patterns in three $<001>_{GPB}$ zones based on the model of Wolverton [12] in Fig. 1(b); (d) Simulated diffraction patterns showing all 6 variants of GPB of Fig. 5(c) upon $[001]_{Al}$.

Sizes of the spots are proportional to the diffraction intensities (I) in which f_{Al}, f_{Cu} and f_{Mg} are the atomic scattering amplitudes.

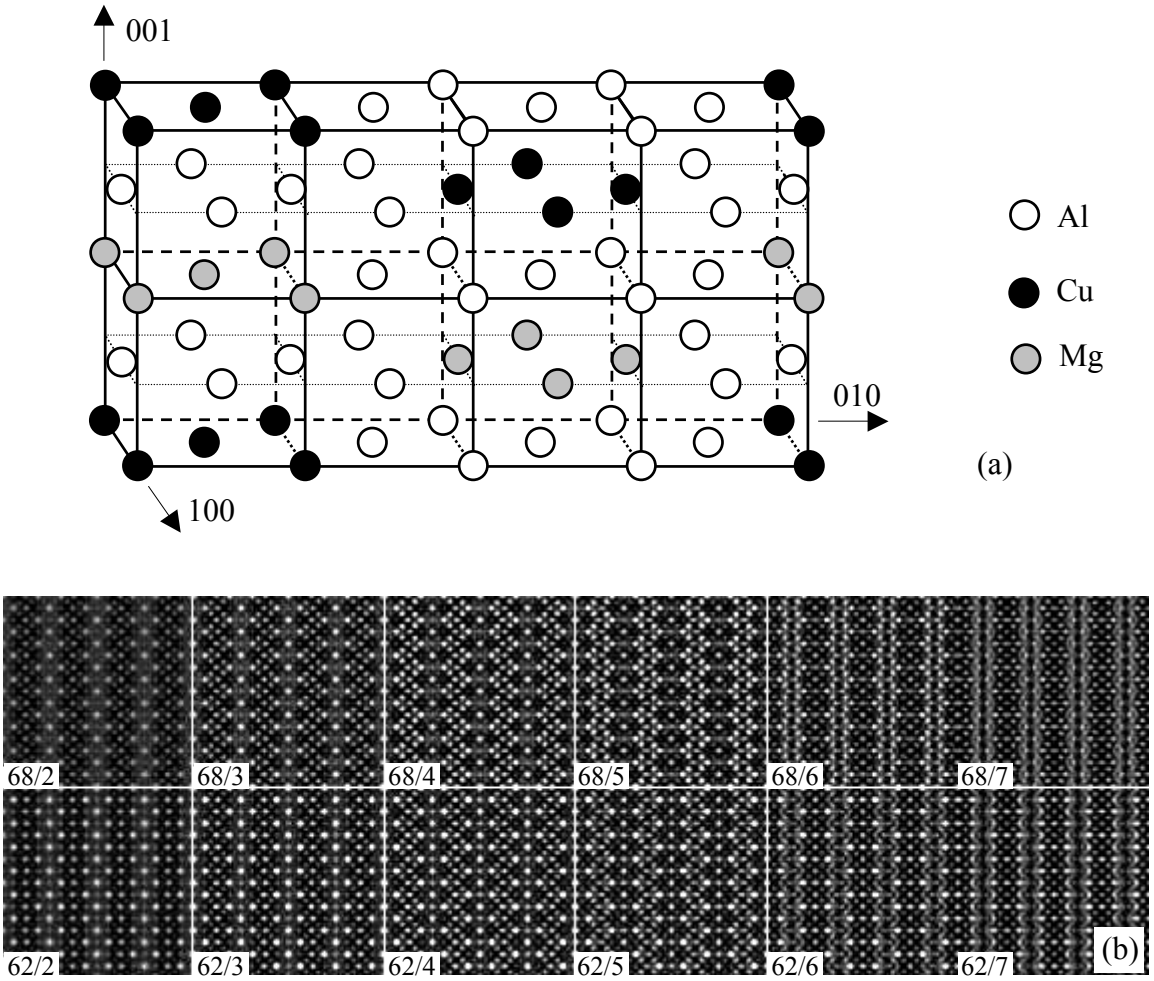

Fig. 6(a) One possible GPB2/S" model for which the simulated HREM images match rectangular region I in Fig. 2(a); (b) HREM simulation along [001] based on the above structures. The numbers before and after the slash symbol "/" represent the defocus and thickness (nm in unit) respectively.

Published in: Materials Science and Engineering A 386(2004) 156-163

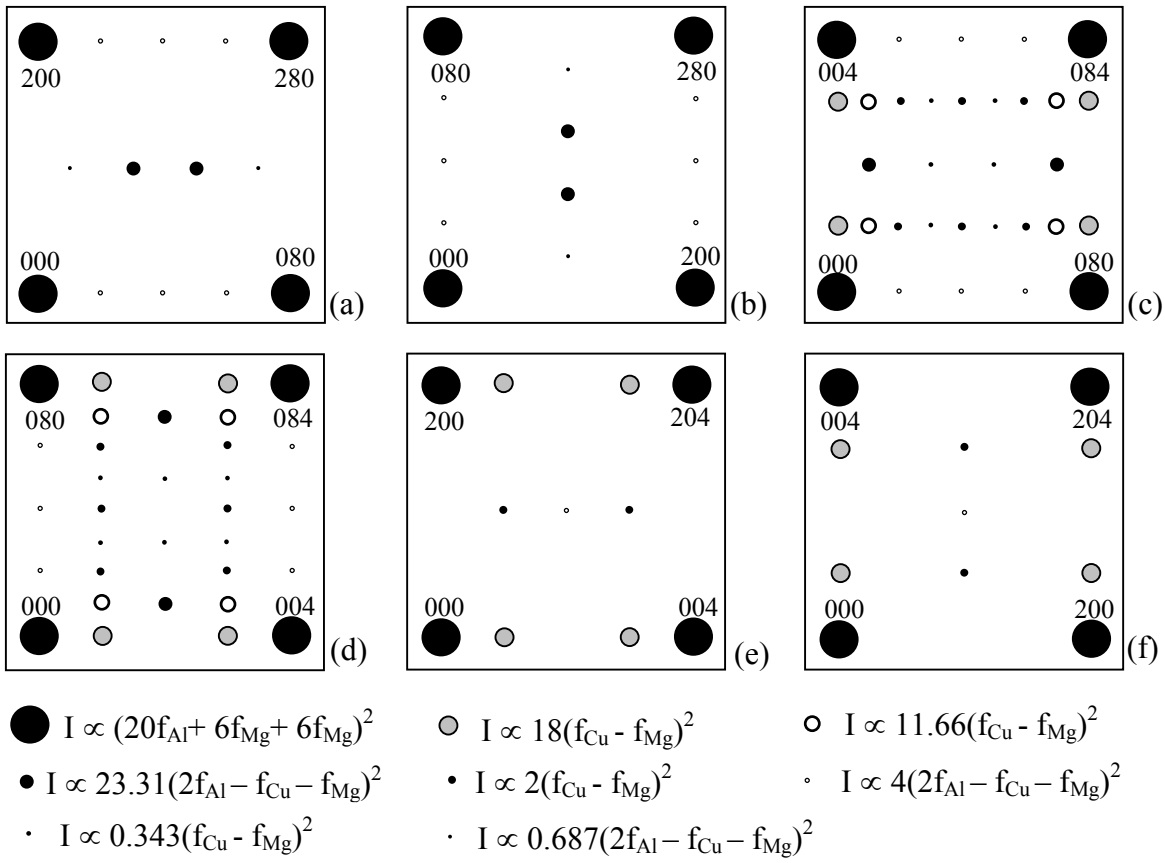

Fig. 7 (a-f) Simulated $<001>_{GPB2/S"}$ patters for all the 6 independent variant of GPB2/S" respectively, based on the model in Fig. 6(a). Sizes of the spots are proportional to the diffraction intensities (I) in which f_{Al}, f_{Cu} and f_{Mg} are the atomic scattering amplitudes. Note that the 4 high intensity spots will coincide with Al spots.

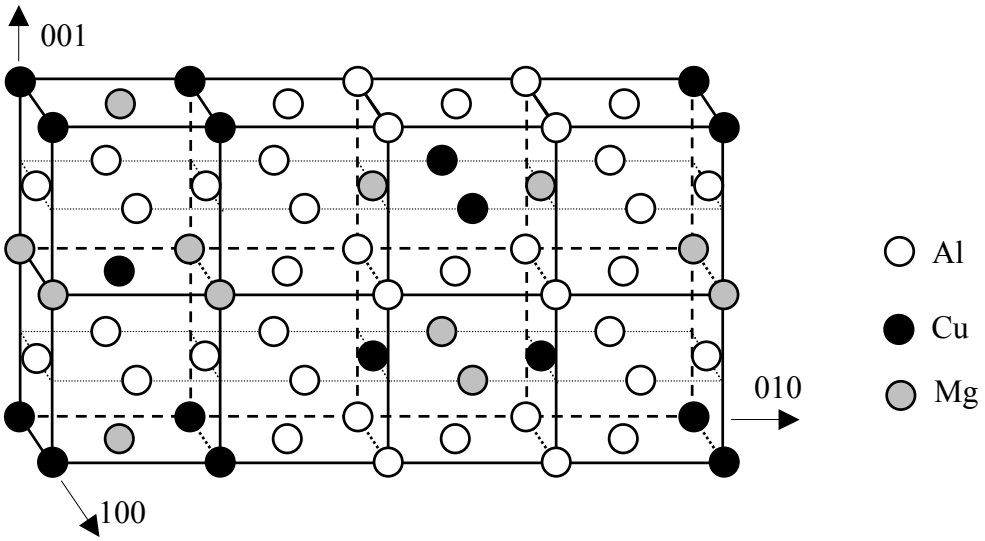

Fig. 8 A modified GPB2/S" model for which the simulated HREM images also match rectangular region I in Fig. 2(a).

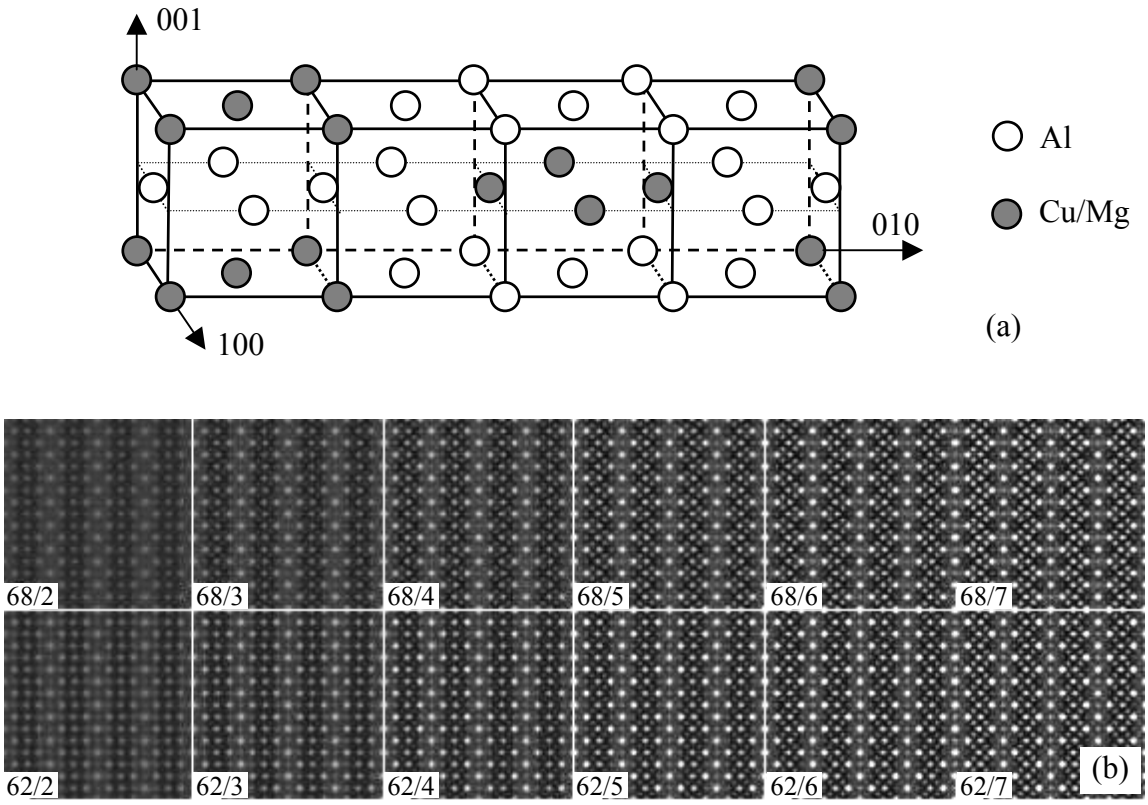

Fig. 9(a) A possible GPB2/S" model for which the simulated HREM images match rectangular region I in Fig. 2(a); (b) HREM simulation along [001] based on the above structures. The numbers before and after the slash symbol "/" represent the defocus and thickness (nm in unit) respectively.

Published in: Materials Science and Engineering A 386(2004) 156-163

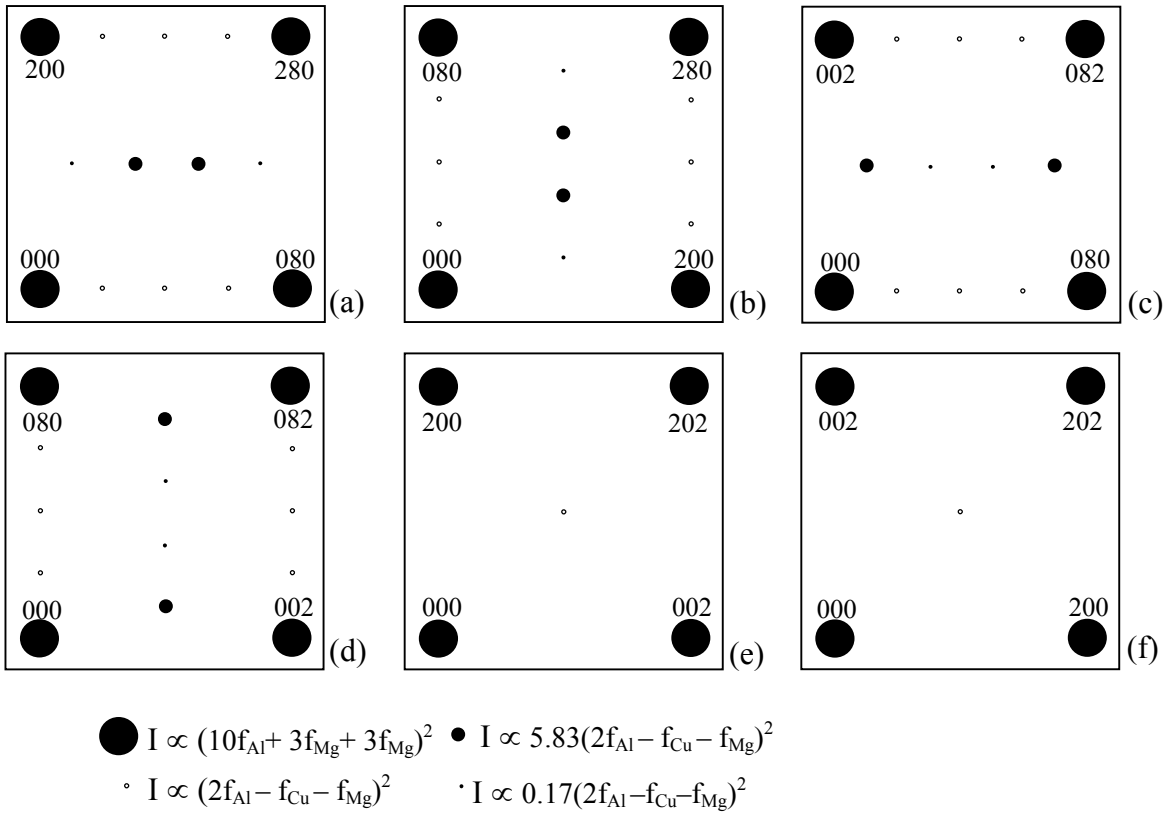

Fig. 10 (a-f) Simulated patters of $<001>_{GPB2/S"}$ for all the 6 independent variants of GPB2/S", based on the model in Fig. 9(a). Sizes of the spots are proportional to the diffraction intensities (I) in which f_{Al}, f_{Cu} and f_{Mg} are the atomic scattering amplitudes. The calculation was based on composition $Al_{10}Cu_3Mg_3$. Note that the 4 high intensity spots will coincide with Al spots.

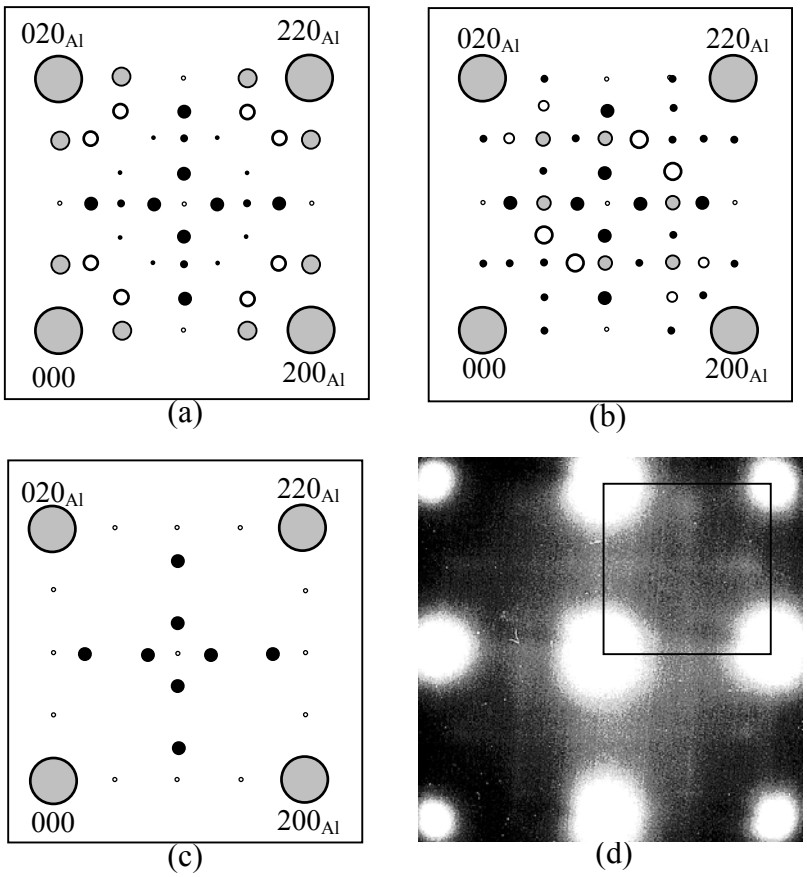

Fig. 11 The complex reflections of all the variants of S" projected on $[001]_{Al}$.
(a) Combination of all the diffractions in Fig. 7 based on model in Fig. 6(a);
(b) Combination of all the diffractions based on model in Fig. 8; (c) Combination of all the diffractions in Fig. 10 based on model in Fig. 9(a); (d) SAD pattern of a 2024 alloy aged at 150ºC for 12h.

References

[1] Y. A. Bagaryatshy, Dokl. Akad. S.S.S.R. 87 (1952) 397, 559.

[2] J. M. Silcock, Journal of the Institute of Metals 89 (1960-61) 203.

[3] L. Reich, S. P. Ringer, K. Hono, Phil. Mag. Lett. 79 (1999) 639.

[4] H. Perlitz, A. Westgren, Arkiv. Kemi. Mineral. Geol. 16B (1943) No13

[5] L.F. Mondolfo, Aluminum alloys-Structure and Properties, Butterworths, London, 1976, p.500.

[6] Y. Jin, C.Z. Li, M.G. Yan, J. Mater. Sci. Lett. 9 (1990) 421.

[7] V. Radmilovic, R. Kilaas, U. Dahmen, G.J. Shiflet, Acta Mater. 47 (1999) 3987.

[8] S. P. Ringer, K. Hono, I. J. Polmear, T. Sakurai, Acta Mater. 44 (1996) 1883.

[9] S. P. Ringer, S. K. Caraher, I.J. Polmear, Scripta Mater. 39 (1998) 1559.

[10] M.J. Starink, J.L. Yan, N. Gao, Mater. Sci. Eng. A, in press.

[11] F. Cuisiat, P. Duval, R. Graf , Scripta Met., 18 (1984) 1051.

[12] C. Wolverton, Acta Mater. 49 (2001) 3129.

[13] R.N. Wilson, P.G. Partridge, Acta Metall. 13 (1965) 1321.

[14] S.P. Ringer, T. Sakurai, I. J. Polmear, Acta Mater. 45 (1997) 3731.

[15] S.C. Wang, M.J. Starink, Proc of Electron Microscopy and Analysis, Oxford, England, 3-5 September, 2003, Inst. Phys. Conf. Ser. No 179: Section 6, p. 277.

[16] T.V.Shchegoleva, N.N.Buinov, Sov. Phy. Cryst. 12 (1967) 552.

[17] A. Charai, T. Walther, C. Alfonso, A. M. Zahra, C. Y. Zahra, Acta Mater. 48 (2000) 2751.

[18] V. Gerold and H. Haberkorn: Z. Metall., 1959, **50**, 568

[19] H. Shih, N. Ho and J.C. Huang, Metall. Materials Trans. A 27 (1996) 2479.

[20] L. Kovarik, P. I. Gouma, C. Kisielowski, S. A. Court and M. J. Mills, Mater. Sci. Eng. A, to be published.

[21] P. Ratchev, B.Verlinden, P. de Smet, P. van Houtte, Acta Mater. 46 (1998) 3523.

[22] A. K. Gupta, P. Gaunt, M. C. Chaturvedi, Phil. Mag. A 55(1987) 375.

[23] P.H. Jouneau, P. Stadelmann, Electron Microscopy image Simulation, http://cimesg1.epfl.ch/CIOLS/crystal1.pl., Centre Interdépartemental de Microscopie Electronique, EPFL, Lausanne, Switzerland.

[24] N. Gao, L. Davin, S. Wang, A. Cerezo, M.J. Starink, Mater. Sci. Forum 396-402 (2002) 923.

[25] A. Guinier, J. Physique Radium 8 (1942) 122.

[26] T. Hahn (ed.), International Tables for Crystallography, volume A: Space-group Symmetry, D. Reidel Publishing Company, Holland/Boston; 1983.

[27] M.J. Starink, J. Yan, Proc. 1st Int. Symp. Metall. Modeling for Al Alloys (M. Tiryakioglu and L.A. Lalli, Eds.), October 12-15, 2003, Pittsburgh, PA, USA, ASM International, Materials Park, Ohio, USA, pp. 119-126.

[28] S.C. Wang, N. Gao, M.J. Starink, unpublished work, University of Southampton, 2003.